Appl. Phys. B 84, 281–287 (2006)
DOI: 10.1007/s00340-006-2252-8

Applied Physics B
Lasers and Optics

S. KACHAN[1,✉]
O. STENZEL[2]
A. PONYAVINA[1]

High-absorbing gradient multilayer coatings with silver nanoparticles

[1] Institute of Atomic and Molecular Physics, National Academy of Sciences of Belarus, 70 Nezavisimosti Avenue, 220072 Minsk, Belarus
[2] Fraunhofer Institute of Applied Optics and Precision Engineering IOF, 07745 Jena, Germany

Received: 3 April 2006
Published online: 23 May 2006 •

ABSTRACT We suggest an efficient way to enhance broadband visible light absorption in multilayer nanostructured systems formed by silver nanoparticle arrays. This approach is based on the explicit use of a gradient change in the parameters of the arrays (such as nanoparticle size or concentration). We analytically derive general conditions of the spectral characteristics of individual arrays which must be satisfied for the realization of highly-absorptive gradient multilayer nanostructured coatings. Two specific types of gradient coatings, (i) with the gradient of the size of the silver nanoparticles in the arrays and (ii) with the gradient of their surface concentration, are numerically studied in detail. The obvious advantages of the size-gradient coatings are revealed, in particular their total thickness of less than a wavelength. Multilayer coatings with a concurrent gradient of both concentration and mean particle size are fabricated from silver island films and their high and broadband absorption is demonstrated experimentally.

PACS 78.67.Pt; 78.67.-n; 73.20.Mf; 42.25.Bs

1 Introduction

Metal-dielectric nanocomposites attract considerable attention as promising materials for the development of new element bases for optoelectronics, bio-sensing, optical data storage and solar energy conversion [1, 2]. Their optical properties are fundamentally based on surface plasmon resonance (SPR) modes of metallic nanoparticles and can be efficiently tailored by nanoparticle materials, sizes, shapes, and concentration.

An additional effective way of SPR control is by spatial arrangement of metal-dielectric nanocomposites, for example, forming the multilayer systems consisting of metallic nanoparticles separated by dielectric layers [3–11]. Currently developed physical [5–12] and chemical [3, 4] techniques for preparation of these metal-dielectric multilayers allow controlling of both the topology of discontinuous metallic layers and the thickness of the dielectric films. In the case of subwavelength thickness of dielectric films the dramatic change in the optical properties of the metal-dielectric multilayers occurs due to the pivotal role of plasmonic-photonic coupling [7, 8]. Subwavelength layer-periodic structures may be regarded as quasi-one-dimensional metallic photonic crystals, where the photonic bandgap occurs under simultaneous realization of electronic and photonic confinements.

In [7, 8] we have theoretically and experimentally considered the multilayer nanostructured systems (MNS), which are stacks composed of identical metallic nanoparticle monolayers separated by dielectric films of equal thickness. Thus, we stacked the single close-packed layers of metallic nanoparticles with identical particle matter, size, concentration and other planar nanostructure parameters. It was shown that with dielectric films of quarter-wave thickness one could reach strong absorption over the SPR spectral range due to reducing both transmission and reflection.

The present paper is aimed at improving the spectral characteristics of the plasmonic-photonic quarter-wave coatings by means of a gradient change of the monolayer parameters. We analyze the conditions of effective enhancement of absorption and suppression of reflection in such gradient multilayer systems, and realize them both theoretically and experimentally for the case of when silver nanoparticle size and/or concentration are changed from monolayer to monolayer in a metal-dielectric stack.

The paper is organized as follows. In Sect. 2 we briefly describe the calculation method applied to obtain the spectral properties of (i) a partially ordered monolayer of metallic nanoparticles and (ii) a multilayer consisting of such nanoparticle monolayers. Modifications in the spectral behavior of a quarter-wave non-gradient multilayer for varying silver nanoparticle sizes or concentrations are presented in Sect. 3. In Sect. 4 we analyze a two-monolayer gradient system and deduce the conditions of simultaneous realization of reduced reflection and stronger absorption compared with non-gradient systems. Optical properties of optimized in this way size-gradient and concentration-gradient multilayers made of silver nanoparticles are theoretically considered in Sect. 5. Experimental implementation of multilayers with a gradient in the mass of silver is presented in Sect. 6.

2 Calculation method

In order to calculate the coefficients of the direct light transmission and specular reflection for metal-dielectric

✉ Fax: +375-17-284-0030, E-mail: kachan@imaph.bas-net.by

MNSs considered in this paper (both non-gradient and gradient), we combine the quasi-crystalline approximation (QCA) applied for calculations of the transmission properties of individual monolayers, with the transfer-matrix technique used for subsequent calculations of the transmission properties of multilayer structures. The QCA method is based on the statistical theory of multiple scattering of waves (STMSW) [13].

2.1 *Quasi-crystalline approximation*

As the first step, which is treated in detail in [14], we deal with the optical properties of a close-packed plane array of spherical particles. The lateral electrodynamic interactions between individual particles of such a monolayer are considered as the interference of multiply scattered waves in a planar partially-ordered arrangement of scatterers. The spatial distribution of particles within each monolayer is specified by the radial distribution function calculated on the assumption of hard spheres [15]. Size-dependence of the dielectric function of small metallic nanoparticles is taken into account in terms of the model of limitation of the electron mean free path [16].

The scattering amplitudes of individual monolayers are determined in the quasi-crystalline approximation of the STMSW, first introduced for close-packed media by Lax [17]. This approximation supposes that fixation of any particle specifies the spatial configuration of the whole array. For random monolayers the closer to the crystalline assembly the structure is, the more justifiable is this assumption. So, we can reasonably apply the QCA to close-packed monolayers as they are characterized by short-range ordering: space sites of neighboring particles are partially correlated due to their finite sizes and high concentration.

Within the QCA, the amplitudes t and r of coherent transmission and reflection coefficients of a close-packed nanoparticle monolayer at normal light incidence takes the form:

$$t = 1 - \frac{\pi}{k^2}\sum_l p_0(2l+1)(\alpha_l+\beta_l)\,,$$
$$r = -\frac{\pi}{k^2}\sum_l p_0(-1)^l(2l+1)(\alpha_l+\beta_l)\,. \qquad (1)$$

Here $k = 2\pi/\lambda$ is the wavenumber in the medium; p_0 is the surface concentration of the particles. Coefficients α_l and β_l are calculated from the linear system of equations containing the Mie coefficients and special functions which are dependent on the radial distribution function and associated with coherent interaction between the particles [14, 18].

2.2 *Transfer-matrix method*

As the second step, we consider the interference between monolayers forming a multilayer. For easy treatment of a stack made of monolayers distinguished in spectral properties, we employ the transfer-matrix technique [19] instead of the more complicated self-consistent procedure used in [14]. This approach implies the statistical independence of particle arrangements for different monolayers that is obviously fulfilled in our case.

Within the T-matrix method the field amplitudes in the left and right sides of a multilayer structure are related by the system T-matrix, which is a product of T-matrices of individual elements, i.e. nanoparticle monolayers ($\hat{T}_i^{\rm m}$) and separating dielectric films ($\hat{T}_i^{\rm f}$). Elements of the transfer matrix of a monolayer are determined by the amplitudes of its coherent transmission and reflection coefficients derived in (1), those of a dielectric film are immediately dependent on its phase thickness δ:

$$\hat{T}_i^{\rm m} = \begin{bmatrix} \frac{1}{t_i} & -\frac{r_i}{t_i} \\ \frac{r_i}{t_i} & \frac{t_i - r_i^2}{t_i} \end{bmatrix}, \quad \hat{T}_i^{\rm f} = \begin{bmatrix} \exp(-{\rm i}\delta_i) & 0 \\ 0 & \exp({\rm i}\delta_i) \end{bmatrix}.$$

For a multilayer made of N different monolayers separated by arbitrary dielectric films the system transfer matrix is:

$$\hat{T}^{\rm multi} = \left(\prod_i^{N-1} \hat{T}_i^{\rm m}\hat{T}_i^{\rm f}\right)\hat{T}_N^{\rm m}\,.$$

Then, we can write the coherent transmittance and reflectance of a multilayer structure as:

$$T = \left|\frac{1}{T_{11}^{\rm multi}}\right|^2, \quad R = \left|\frac{T_{21}^{\rm multi}}{T_{11}^{\rm multi}}\right|^2. \qquad (2)$$

Recalling that coherent T and R correspond to the coefficients of direct transmission and specular reflection, measured in the case of small-angular detection.

3 Non-gradient multilayer nanostructured systems

Let us now consider the calculated modifications of the spectral properties of the quarter-wave non-gradient MNS (see Fig. 1) caused by the change of either size or surface concentration of nanoparticles in monolayers. To be specific, we assume throughout this paper that nanoparticles are made from silver (using optical constants taken from [20]), and that dielectric films, as well as the host media of monolayers, are made from Al_2O_3 (refractive index $n \approx 1.75$ for optical wavelengths, where dispersion is neglected). In all cases we deal

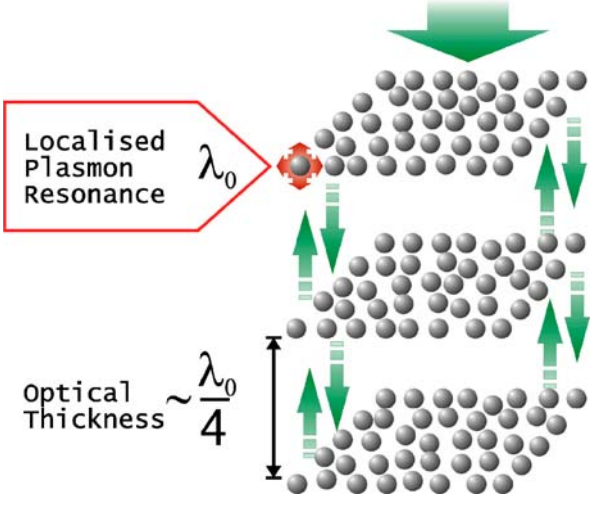

FIGURE 1 Schematic illustration of a quarter-wave multilayer nanostructured system made of metallic nanoparticle monolayers

with normal incident light. The quarter-wave optical thicknesses of dielectric films are adjusted to the peak wavelength λ_0 of the SPR band of monolayers. Besides, we describe a concentration change of particles in a monolayer in terms of the particle volume fraction $f = p_0\pi d^2/6$ that gives the relation of the volume occupied by particles with diameter d to the monolayer volume.

In Fig. 2 we plot the spectral characteristics of three non-gradient multilayers, each consisting of three identical monolayers of spherical silver nanoparticles, separated from each other by a dielectric film of a quarter-wave optical thickness. The structures shown in Fig. 2a and 2c have sufficiently high absorptance and low reflectance and, therefore, can be effectively used as the light-absorbing coatings. For broadband applications however, the problem is that the spectral widths of their absorption bands are rather narrow. In principle, it is possible to make them much broader by increasing either the surface concentration (compare Fig. 2a with 2b) or the size (compare Fig. 2c with 2b) of the particles in the monolayers. However, in this way we simultaneously increase the undesirable reflections from such a multilayer structure over the SPR spectral range. This behavior of the non-gradient multilayers is caused by the optical response of isolated monolayers: the reflection from a monolayer at the SPR frequency is an increasing function of particle concentration or size, as it is demonstrated in Fig. 3 by calculations performed in the QCA.

Nevertheless, if we adhere to an idea that is used in the dielectric antireflection coatings with gradient-index profiles [21, 22], we can try to utilize the increasing reflection from individual monolayers in order to reduce the reflectance of a multilayer. In the case of gradient-index dielectric coatings the gradual transition from one subwavelength slice to another (accompanied by an increase both in refractive index and in reflectance of a slice) considerably reduces the reflection from the whole system. By analogy we can suggest that the gradient multilayer composed from monolayers with a growing concentration or/and size of metallic nanoparticles, could also have reduced reflectance due to gradually increasing reflection from monolayers. So, this implementation could permit us to remove the parasitic reflection and to get the desired high and broadband absorption in nanostructured multilayer coatings.

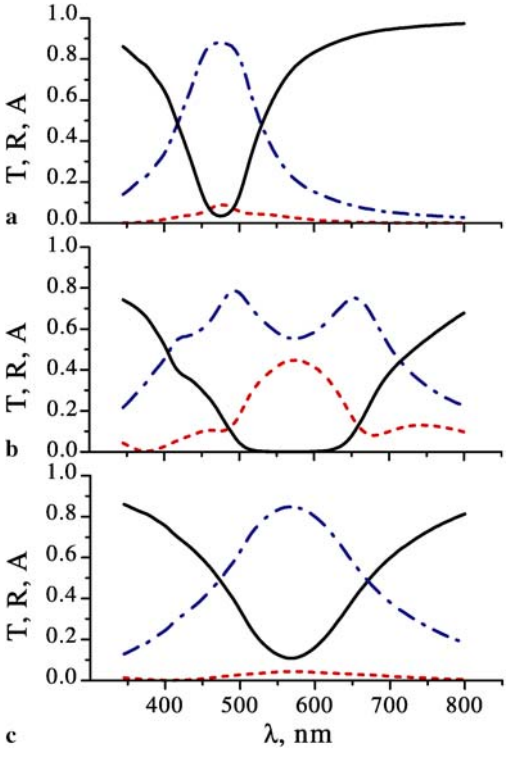

FIGURE 2 Calculated transmittance (*solid lines*), reflectance (*dashed lines*) and absorptance (*dot-dashed lines*) spectra of a non-gradient quarter-wave stack of 3 close-packed silver nanoparticle monolayers for different monolayer parameters: (**a**) $d = 15$ nm; $f = 0.13$; (**b**) $d = 15$ nm; $f = 0.4$; (**c**) $d = 5$ nm; $f = 0.4$

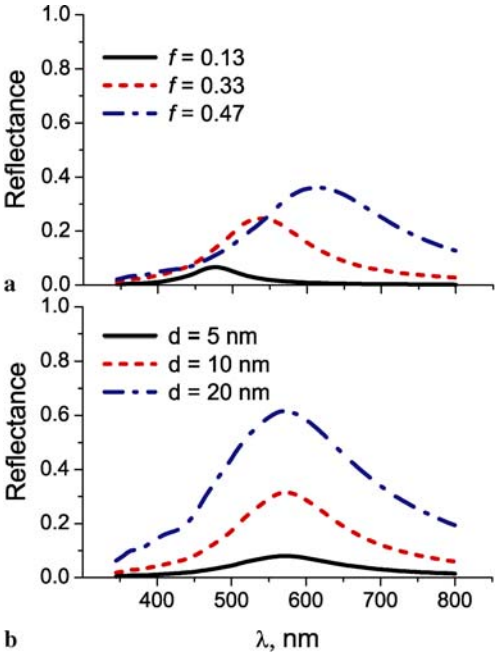

FIGURE 3 Calculated reflectance spectra of close-packed Ag monolayers different in (**a**) particle volume fraction (at constant nanoparticle sizes $d =$ 10 nm); (**b**) nanoparticle sizes (at constant particle volume fraction $f = 0.4$)

4 Analysis of a two-monolayer gradient system

Let us analyze the conditions under which the gradient MNS does have both larger absorptance and smaller reflectance compared with non-gradient MNS. To get an analytical insight into the problem, we shall first consider the simplest gradient system which consists of two nanoparticle monolayers separated by a dielectric spacer, as it is shown in Fig. 4. Since such a structure is the basis element of multilayer gradient systems, the results obtained from the two-monolayer system should be applicable, in some approximation, to the multilayer systems, as well.

To exclude the effects of interference associated with the dielectric/substrate and dielectric/air interfaces from our theoretical analysis of the basis element, we assume that the ambient materials are identical to the spacer material. Supposing normal incidence of a plane electromagnetic wave on the stack and neglecting the coupling of evanescent waves of neighbouring monolayers, we define the ampli-

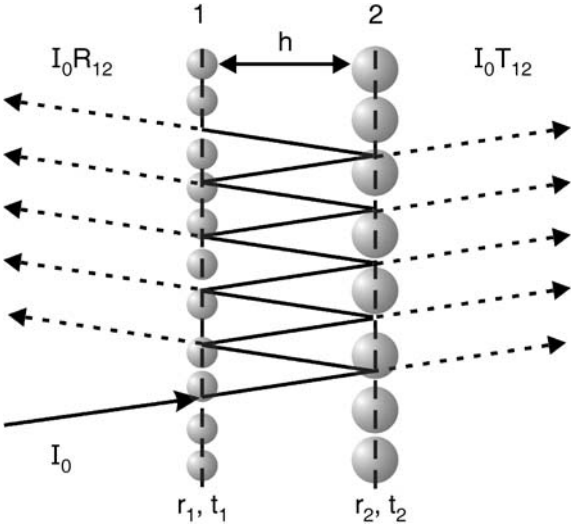

FIGURE 4 Interference scheme of plane wave interaction with a two-monolayer gradient system

tude transmission and reflection coefficients of the 1-st and 2-nd monolayers as $t_1 = |t_1| \exp(\mathrm{i}\varphi_1^t)$, $r_1 = |r_1| \exp(\mathrm{i}\varphi_1^r)$ and $t_2 = |t_2| \exp(\mathrm{i}\varphi_2^t)$, $r_2 = |r_2| \exp(\mathrm{i}\varphi_2^r)$, respectively. Here φ_i^t and φ_i^r are the phases of transmission and reflection coefficients of i-th monolayer.

Taking into account absorption inside both monolayers and all orders of multiple scattering of light between them, we can write the amplitude transmission and reflection coefficients of the two-monolayer system with physical spacer thickness h as the following:

$$t_{12} = \frac{t_1 t_2 \exp(\mathrm{i}kh)}{1 - r_1 r_2 \exp(2\mathrm{i}kh)} ,$$
$$r_{12} = r_1 + \frac{r_2 t_1^2 \exp(2\mathrm{i}kh)}{1 - r_1 r_2 \exp(2\mathrm{i}kh)} . \quad (3)$$

These expressions are reduced to the Airy's formulae for a thin dielectric film [23] in the case when (i) the absorption in monolayers is neglected and (ii) the amplitudes of the reflection coefficients of monolayers are connected by the relationship $r_1 = -r_2$, as a result of the π-phase jump for reflection from the external and internal boundaries of a dielectric film.

Neglecting the diffuse light scattering by nanostructured monolayers (i.e., supposing the absorption by i-th monolayer is equal to $A_i = 1 - T_i - R_i$, where $T_i = |t_i|^2$ and $R_i = |r_i|^2$ are the energetic coefficients of direct transmission and specular reflection of the monolayer, accordingly) we can find the relations between phases of the amplitude coefficients. Provided the two-monolayer system absorption $A_{12} = 1 - |t_{12}|^2 - |r_{12}|^2$ is equal to zero irrespective of distance between the monolayers, in the case when both monolayers are non-absorbing $A_1 = A_2 = 0$, we derive the relation of phases for an individual weakly absorbing monolayer as:

$$\varphi_i^r = \varphi_i^t \pm \pi/2 . \quad (4)$$

It should be noted that this relation changes as the absorption A_i by the monolayer increases and thus consideration of highly absorbing monolayers would require an additional analysis. Then we substitute (4) into (3) and from the condition of the desired minimum of the two-monolayer system reflection we determine the relation between the phase thickness of a dielectric spacer and the phases of the amplitude reflection coefficients of monolayers as:

$$\varphi_1^r + \varphi_2^r = 2(\pi m - kh) , \quad m = 0, \pm 1 \ldots \quad (5)$$

Finally, employing (3)–(5), we obtain for weakly absorbing monolayer relatively simple expressions for the transmission, reflection and absorption coefficients of our elementary two-monolayer gradient system in the case when a choice of spacer thickness h minimizes reflection from the whole system ($hn \approx \lambda/4$):

$$T_{12} = \frac{T_1 T_2}{(1 - \sqrt{R_1 R_2})^2} ,$$
$$R_{12} = \left[\frac{\sqrt{R_1} - \sqrt{R_2}(1 - A_1)}{1 - \sqrt{R_1 R_2}} \right]^2 ,$$
$$A_{12} = A_1 + \frac{T_1 (A_2 + A_1 R_2)}{(1 - \sqrt{R_1 R_2})^2} . \quad (6)$$

From (6) it is evident that the reflection coefficient of any non-gradient two-layer absorbing system with quarter-wave interlayer distance $R_{ii} = R_i A_i^2 (1 - R_i)^{-2}$ could be less than the reflection coefficient of a single monolayer R_i but could not be reduced to zero. Only the gradient stack gives the possibility of completely eliminating reflection at $R_1 = R_2 (1 - A_1)^2$.

The analysis of (6) shows that in order to obtain the gradient system having, at the matching frequency, smaller reflectance and higher absorptance than both non-gradient systems (1-st and 2-nd non-gradient systems composed from identical monolayers of type 1 and of type 2, respectively), the monolayers should satisfy some necessary conditions:

$$R_2 > R_1 , \; A_2 \le A_1 , \; T_2 \le T_1 , \quad (7)$$

The limitation $T_2 \le T_1$ can be also rewritten (accounting for all of these conditions) in the equivalent but sometimes more convenient form: $\Delta R > \Delta A$, where $\Delta R = |R_2 - R_1|$, and $\Delta A = |A_2 - A_1|$. Thus, the growth in reflection of the second monolayer should be more pronounced than the decrease in absorption.

These conditions are supported by the following simple physical considerations: for larger reflections from the second monolayer, the intensities of the beams reflected from the first and second monolayers become comparable, that leads to a higher efficiency of a destructive (for a quarter-wave distance between monolayers) light interference in the system and, therefore, suppresses the total reflection from the gradient system. If in addition, the absorption of the first monolayer exceeds the absorption of the second monolayer, then the light beam is not only less attenuated after a bounce onto the second monolayer (in comparison with the 1-st non-gradient system), but is also more strongly absorbed by this first monolayer (in comparison with the 2-nd non-gradient system).

It is also obvious from (6) that while transmittance of the gradient system is invariant to a direction change of normal light incidence (i.e., for wave vectors $\boldsymbol{k}$ and $-\boldsymbol{k}$), the reflection and absorption coefficients, in contrast, are different for

opposite directions. For the gradient MNS which meets the conditions of (7), the abrupt increase in reflection and, respectively, the decrease in absorption takes place as the light incidence direction changes from forward (along the gradient vector) to reverse. Besides, this spectral difference becomes more significant when the ratio R_2/R_1 grows.

5 Size-gradient and concentration-gradient multilayer nanostructured systems

Here we shall theoretically consider two possible realizations of the gradient multilayer system: (i) with a gradual change of nanoparticle surface concentration from one monolayer to another, provided that all particles in the system have identical size (we shall refer to such systems in what follows as to the concentration-gradient MNSs), and (ii) with graded sizes of the nanoparticles, assuming that the metal concentration remains constant for all monolayers of the system (size-gradient MNSs). Note that in both gradient systems the mass of metal grows from monolayer to monolayer.

We have already mentioned that for metal nanoparticles assembled in a monolayer, both the increase in their size and the increase in their concentration enhances the reflectance R_{λ_0} at the monolayer SPR wavelength λ_0 (see Fig. 3). At the same time, the monolayer transmittance T_{λ_0} steadily decreases, as we already showed in [24]. Aside from these quantitative changes in peak value of the SPR bands, another important feature is the spectral behaviour of the SPR wavelength λ_0. It remains approximately constant if we vary the size of the nanoparticles in the monolayers with the same metal volume fraction f otherwise, it exhibits a strong red shift if we vary their concentration provided we have fixed sizes. Note that such a simple tendency is intrinsic only for small-size nanoparticles, i.e. particles which can be described in terms of the quasistatic approximation, when the electric dipole-dipole interaction dominates the electrodynamic coupling between scatterers.

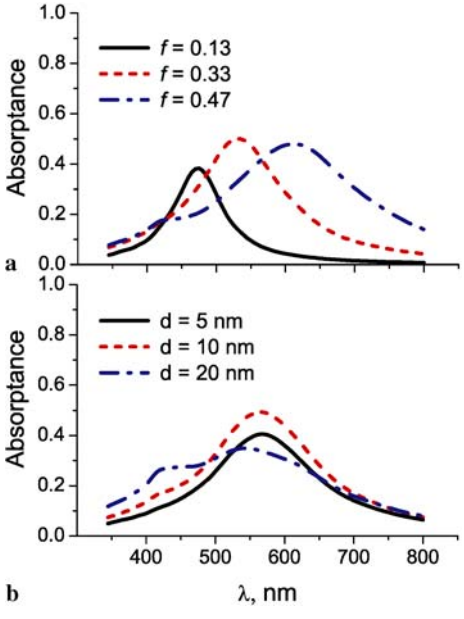

FIGURE 5 Calculated absorption spectra of close-packed Ag monolayers different in (**a**) particle volume fraction (at constant nanoparticle sizes $d =$ 10 nm); (**b**) nanoparticle sizes (at constant particle volume fraction $f = 0.4$)

As one can observe from Fig. 5, the resonance absorption function $A_{\lambda_0} = 1 - T_{\lambda_0} - R_{\lambda_0}$, calculated using the QCA, exhibits a substantially non-monotonic (having a maximum) dependence on nanoparticle size (see Fig. 5a) or concentration (see Fig. 5b) in close-packed silver monolayers. Thus, taking into account the behaviours of T_{λ_0} and R_{λ_0}, we can conclude that in a certain particle size or concentration interval all conditions (7) are satisfied in the vicinity of λ_0 for neighbouring monolayers.

However, it should be emphasised that the size-gradient MNSs have a substantial advantage in meeting the conditions (7) compared with the concentration-gradient MNSs. Quasistable spectral positions of the SPR frequency in the monolayers with a constant metal volume fraction, but different sizes of metallic particles over the electrostatic range, (see Fig. 3b and Fig. 5b) results in a strong overlap of the SPR bands of the individual monolayers in a size-gradient multilayer system. It helps to satisfy the conditions (7) in a wide spectral region combining monolayers with particles of essentially different size.

In contrast, the red shift of the SPR wavelength in monolayers of the concentration-gradient MNSs leads to the situation when the conditions (7) can be satisfied only in a narrow spectral interval and for a small change of concentration in neighbouring monolayers. For example, from Fig. 3a we can see that for monolayers with metal concentrations $f = 0.33$ and $f = 0.47$ the condition $R_2 > R_1$ is fulfilled at wavelengths greater than 545 nm, but from Fig. 5a it is obvious that $A_2 \leq A_1$ at wavelengths of less than 560 nm. So, the optimization range of this gradient system is quite impractical.

Frequency matching of separate monolayers in the size-gradient MNS enables one to achieve extraordinarily high absorbtion with just a few particle monolayers in the stack. In Fig. 6 we present the calculated absorption and reflection spectra for quarter-wave size-gradient MNSs made from only two close-packed monolayers of silver nanoparticles: the diameter of the particles in the first monolayer is 5 nm and in the second it is 15 nm. The concentration in both monolayers remains constant and corresponds to $f = 0.33$. As one can see from this figure, when the incident beam is coming from the side of the first monolayer, the absorption in this gradient structure is appreciably higher (97% at $\lambda_0 = 570$ nm) than for both non-gradient structures: made of either two monolayers with 5 nm particles (absorbs 75%) or two monolayers with 15 nm particles (absorbs only 55%). Higher reflectance of the second monolayer in comparison to the first monolayer allows us to effectively suppress the reflection from this two-monolayer gradient MNS in the vicinity of λ_0 without any additional antireflection coating. For the inverse direction of the incident beam (from the side of the second monolayer), we observe an abrupt change of the optical response (A, R) that reaches almost half the incident intensity (47%).

For the concentration-gradient MNSs, to gain an advantage over non-gradient systems, one should compensate the requirement of a small change in concentration within neighbouring monolayers (which follows for such systems from the conditions (7)) by using a sufficiently large number of monolayers. Figure 7 shows the calculated spectral properties of

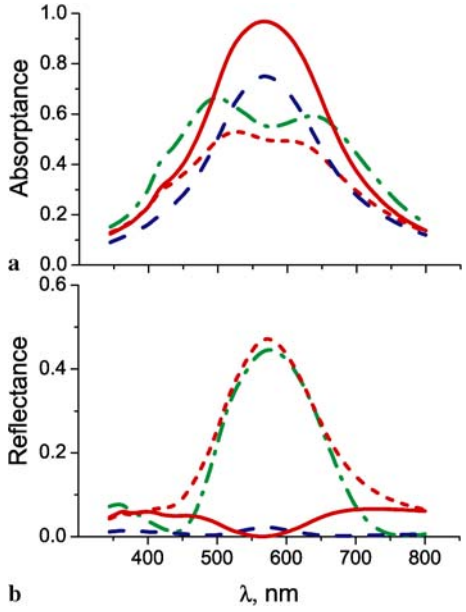

FIGURE 6 Calculated absorption (**a**) and reflection (**b**) spectra for three different quarter-wave structures composed of two close-packed Ag nanoparticle monolayers ($f = 0.4$). *Solid lines* correspond to the size-gradient system with d increasing from 5 nm to 15 nm. *Dotted lines* correspond to the case of inverse light incidence on the size-gradient system. *Dashed* and *dot-dashed lines* describe the non-gradient systems with $d = 5$ nm and $d = 15$ nm, respectively

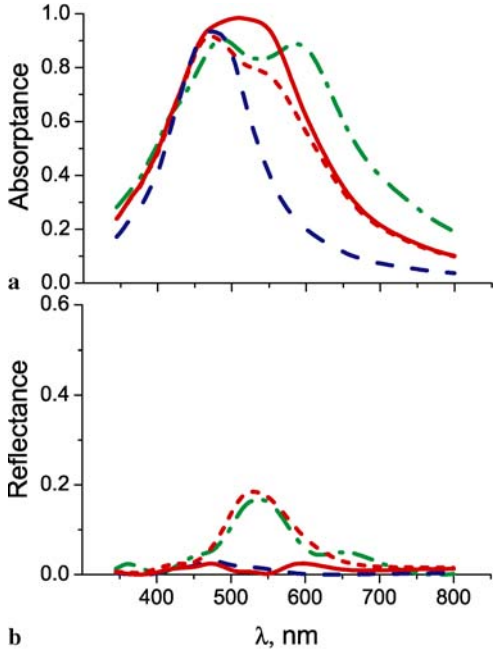

FIGURE 7 Calculated absorption (**a**) and reflection (**b**) spectra for three different quarter-wave structures composed of five close-packed Ag nanoparticle monolayers ($d = 10$ nm). *Solid lines* correspond to the concentration-gradient system with f increasing from 0.13 to 0.33. *Dotted lines* correspond to the case of inverse light incidence on the concentration-gradient system. *Dashed* and *dot-dashed lines* describe non-gradient systems with $f = 0.13$ and $f = 0.33$, respectively

the concentration-gradient stack containing five monolayers of silver nanospheres ($d = 10$ nm) with a uniform increase of the particle volume fraction f from 0.13 till 0.33. The thicknesses of quarter-wave films were adjusted to the plasmon wavelength of the most dense monolayer (λ_0=535 nm). The spectra of non-gradient systems with low ($f = 0.13$) and high ($f = 0.33$) contents of the same particles in monolayers are also represented in this figure.

One can see that this concentration-gradient MNS combines negligibly small (< 3%) reflectance over the SPR range with a noticeable advantage in absorption ability. Absorption in the vicinity of the SPR peak is higher for this gradient MNS compared to both non-gradient systems. Integral absorption of the gradient system is a little less than that of the dense non-gradient system, but it is much larger than integral absorption of the rare non-gradient system, which is comparable with the gradient MNS in reflectance.

It should be emphasized that at low frequencies the optimized concentration-gradient MNSs always absorb more strongly than the non-gradient systems made of rare monolayers, but less than the non-gradient systems made of dense monolayers. This disadvantage of concentration-gradient systems is related to the red shift of plasmon absorption bands with growing particle concentrations. Due to this shift the condition $A_2 \leq A_1$, implicated in (7), is always broken at low frequencies for neighbouring monolayers of these systems.

6 Experimental

For practical implementation of a gradient multilayer system, we alternately performed electron-beam evaporation of a dielectric fraction and thermal evaporation of a metallic fraction as it was described in more detail elsewhere [25]. By this approach, we prepared MNSs consisting of three, four and five silver island films, separated by the quarter-wave Al_2O_3 layers. The nanostructured silver films obtained are characterized by a rather significant disorder in the sizes and shapes of the metallic islands. Figure 8a shows an example of a transmission electron microscopy (TEM) image of a close-packed island film. In the prepared multilayer systems the mass of silver grows from one island film to another towards the substrate. This growth is caused by both the increase in surface concentration of islands and the increase in their mean size, as it is shown in the scanning electronic microscopy (SEM) cross-sectional image (see Fig. 8b).

The topological disorder in sizes and shapes of particles considerably broadens the plasmonic resonance bands in spectra of separate island films and promotes attaining of the favourable conditions for effective absorption enlargement and reflection suppression in gradient MNSs. In Fig. 8c we present spectral dependencies of the transmittance, reflectance and absorptance of the gradient system which includes five silver island films. The inset in Fig. 8c shows the dependence of the absorption on the number of layers in the fabricated gradient MNS at the SPR wavelength. One can see that in the SPR region the gradient system reflects less than 1%, while reflection from a separate island film reaches 43%. The light absorption in this structure achieves 98.5% at 560 nm against 39% in a single island film, and it is more than 60% over the whole optical range. The peak value of the absorption band as well as its bandwidth tends to grow as the number of island films increases.

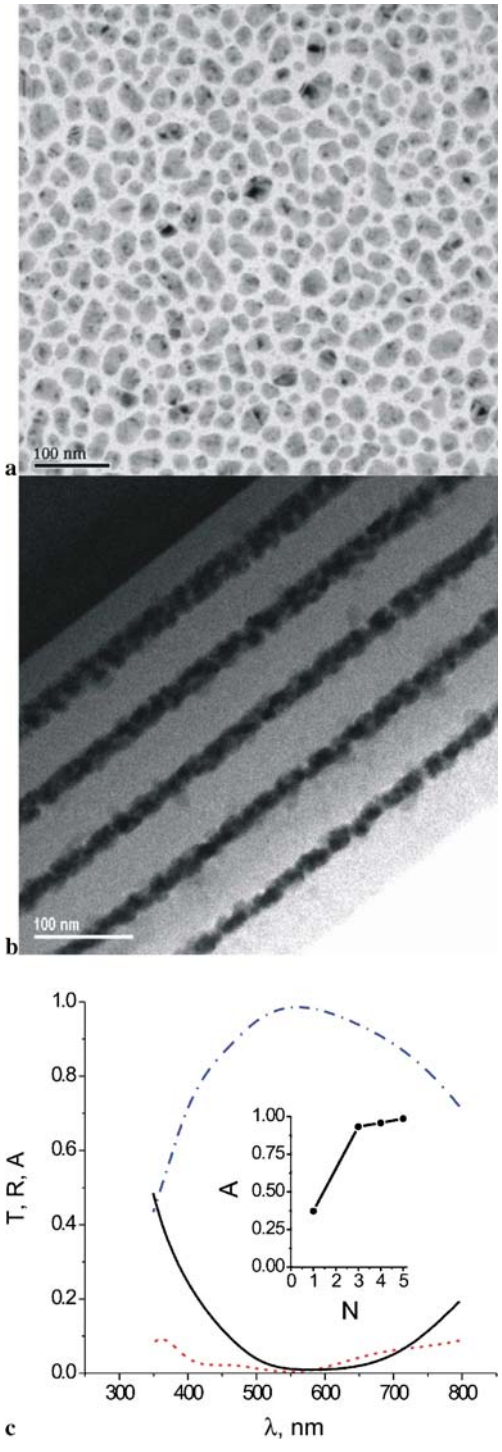

FIGURE 8 Electron microscopy images of (**a**) a silver island film in a Al_2O_3 matrix (*top view*) and (**b**) gradient multilayer coating with five silver island films separated by Al_2O_3 quarter-wave films on a quartz substrate (*side view*); (**c**) transmittance (*solid line*), reflectance (*dashed line*) and absorptance (*dot-dashed line*) spectra for this gradient multilayer structure. The *inset* shows the dependence of the absorption value on the number of island films at $\lambda = 560$ nm

7 Conclusions

In summary, in this work we suggested and substantiated the usage of a gradient change of parameters of nanoparticle monolayers (such as nanoparticle size or concentration) as an elegant way to suppress light reflection and to efficiently enhance broadband absorption in plasmonic quarter-wave multilayer nanostructured systems over the visible range. We theoretically analyzed general conditions of the spectral characteristics of individual monolayers which must be satisfied for realization of highly-absorptive gradient multilayer nanostructured coatings.

Two specific types of the gradient coatings, (i) with the gradient of the size of silver nanoparticles in monolayers and (ii) with the gradient of their concentration, were considered in detail by a method combining the quasi-crystalline approximation and the transfer-matrix technique. For the reverse light incidence direction the dramatic change in absorption and reflection properties of optimized gradient systems was established. To experimentally support our results we fabricated multilayer structures consisting of silver island films with the mass gradient of silver (i.e. a simultaneous increase in particle concentration and mean size). High and broadband absorption of such gradient coatings was successfully verified.

ACKNOWLEDGEMENTS The theoretical part of this work was supported by the International Scientific and Technical Center from Grant #B-276-2. The experimental part was sponsored by the TMWFK (Thüringen, Germany) in terms of the NOB grant.

The authors are grateful to Hanno Heiße, Gisela Kühne, and Petra Heger (all IOF) for experimental work, Prof. Ute Kaiser (Ulm University, Germany) for TEM investigations, as well as to Prof. Norbert Kaiser (IOF) and Dr. Sergei Mingaleev (Karlsruhe University, Germany) for fruitful discussions. O. Stenzel thanks the Deutsche Forschungsgemeinschaft (DFG) for sponsoring a scientific stay in Minsk at the Institute of Atomic and Molecular Physics.

REFERENCES

1 V.M. Shalaev (Ed.), *Optical Properties of Nanostructured Random Media* (Springer, Berlin, 2002)
2 E. Hutter, J.H. Fendler, Adv. Mater. **16**, 1685 (2004)
3 J. Schmitt, G. Decher, W.J. Dressik, S.L. Brandow, R.E. Geer, R. Shashidar, J.M. Calvert, Adv. Mater. **9**, 61 (1997)
4 T. Cassagneau, J.H. Fendler, J. Phys. Chem. B **103**, 1789 (1999)
5 M. Takakuwa, K. Baba, M. Miyagi, Opt. Lett. **21**, 1195 (1996)
6 K. Baba, K. Yamaki, M. Miyagi, Appl. Opt. **38**, 2564 (1999)
7 S.M. Kachan, A.N. Ponyavina, Proc. SPIE **4705**, 88 (2002)
8 A.D. Zamkovets, S.M. Kachan, A.N. Ponyavina, N.I. Silvanovich, Appl. Spectrosc. **70**, 540 (2003)
9 H.B. Liao, W. Wen, G.K.L. Wong, J. Appl. Phys. **93**, 4485 (2003)
10 H. Liao, W. Lu, S. Yu, W. Wen, G.K.L. Wong, J. Opt. Soc. Am. B **22**, 1923 (2005)
11 T. Girardeau, S. Camelio, D. Babonneau, J. Toudert, A. Barranco, Thin Solid Films **455–456**, 313 (2004)
12 J.-P. Barnes, N. Beer, A.K. Petford-Long, A. Suarez-Garcia, R. Serna, D. Hole, M. Weyland, P.A. Midgley, Nanotechnology **16**, 718 (2005)
13 A. Ishimaru, *Wave Propagation and Scattering in Random Media* (Academic Press, New York, 1978), p. 317
14 A. Ponyavina, S. Kachan, N. Silvanovich, J. Opt. Soc. Am B **21**, 1866 (2004)
15 J. Ziman, *Models of Disorder* (Cambridge University Press, Cambridge, 1979)
16 U. Kreibig, C.V. Fragstein, Z. Phys. **224**, 307 (1969)
17 M. Lax, Phys. Rev. **85**, 621 (1952)
18 K.M. Hong, J. Opt. Soc. Am. **70**, 821 (1980)
19 C.C. Katsidis, D.I. Siapkas, Appl. Opt. **41**, 3978 (2002)
20 E.D. Palik (Ed.), *Handbook of Optical Constants of Solids* (Academic Press, New York, 1991)
21 M.J. Minot, J. Opt. Soc. Am. **66**, 515 (1976)
22 H. Sankur, W.H. Southwell, Appl. Opt. **23**, 2770 (1984)
23 M. Born, E. Wolf, *Principles of Optics* (MacMillan, New York, 1964), p. 254
24 S.M. Kachan, A.N. Ponyavina, J. Phys.: Condens. Matter **14**, 103 (2002)
25 P. Heger, O. Stenzel, N. Kaiser, Proc. SPIE **5250**, 21 (2004)